Inorg. Chem. **2005**, *44*, 5042–5046

Synthesis, Structure, and Magnetic Properties of the Layered Copper(II) Oxide $Na_2Cu_2TeO_6$

Jianxiao Xu,[†] Abdeljalil Assoud,[†] Navid Soheilnia,[†] Shahab Derakhshan,[†] Heather L. Cuthbert,[‡] John E. Greedan,[‡] Mike H. Whangbo,[§] and Holger Kleinke*,[†]

Department of Chemistry, University of Waterloo, Waterloo, Ontario, Canada N2L 3G1, Department of Chemistry and the Brockhouse Institute for Materials Research, McMaster University, Hamilton, Ontario, Canada L8S 4M1, and Department of Chemistry, North Carolina State University, Raleigh, North Carolina 27695-8204

Received February 22, 2005

A new quaternary layered transition-metal oxide, $Na_2Cu_2TeO_6$, has been synthesized under air using stoichiometric (with respect to the cationic elements) mixtures of Na_2CO_3, CuO, and TeO_2. $Na_2Cu_2TeO_6$ crystallizes in the monoclinic space group *C*2/*m* with $a = 5.7059(6)$ Å, $b = 8.6751(9)$ Å, $c = 5.9380(6)$ Å, $\beta = 113.740(2)°$, $V = 269.05(5)$ Å^3, and $Z = 2$, as determined by single-crystal X-ray diffraction. The structure is composed of $^2_\infty[Cu_2TeO_6]$ layers with the Na atoms located in the octahedral voids between the layers. $Na_2Cu_2TeO_6$ is a green nonmetallic compound, in agreement with the electronic structure calculation and electrical resistance measurement. The magnetic susceptibility shows Curie–Weiss behavior between 300 and 600 K with an effective moment of 1.85(2) μ_B/Cu^{II} and $\Theta_c = -87(6)$ K. A broad maximum at 160 K is interpreted as arising from short-range one-dimensional antiferromagnetic correlations. With the aid of the technique of magnetic dimers, the short-range order was analyzed in terms of an alternating chain model, with the surprising result that the stronger intrachain coupling involves a super-superexchange pathway with a Cu–Cu separation of >5 Å. The J_2/J_1 ratio within the alternating chain refined to 0.10(1), and the spin gap is estimated to be 127 K.

Introduction

Ternary and higher cuprates are an in part thoroughly investigated class since the CuO_2 layers form the backbone of many high-T_C superconductors including $YBa_2Cu_3O_7$ and related materials.[1,2] In contrast to this, the quaternary cuprate−tellurates with d^9-Cu^{II} ions are basically unexplored; ternary examples for this class are Cu^{II}Te^{VI}O$_4$[3] and Cu$^{II}_3$Te^{VI}O$_6$.[4] A few quaternaries are known, including Sr_2CuTeO_6[5] and Ba_2CuTeO_6.[6] Sr_2CuTeO_6 and the high-pressure modification of Ba_2CuTeO_6 are (tetragonally distorted) ordered perovskites exhibiting two-dimensional antiferromagnetism arising via superexchange from the d^9 system of Cu^{II}.[7] The tetragonal distortion is a consequence of the Jahn−Teller effect causing a [4 + 2] coordination of the Cu^{II} atoms. The magnetic properties of cuprates are strongly effected by this pronounced orbital ordering, and often the results are surprising. We succeeded in synthesizing the first example with an alkali metal, forming a new layered compound. With this contribution we present its crystal structure and electronic structure, as well as transport and magnetic properties.

Experimental Section

Synthesis. Phase pure $Na_2Cu_2TeO_6$ was prepared by starting from 1 mmol of Na_2CO_3 (Merck, powder, purity 99.5%), 2 mmol of CuO (BDH Chemicals, powder, purity 99.0%), and 1 mmol of TeO_2 (Fisher Scientific, powder, purified) under air, i.e., oxidizing

* Author to whom correspondence should be addressed. E-mail: kleinke@uwaterloo.ca.
[†] University of Waterloo.
[‡] McMaster University.
[§] North Carolina State University.

(1) Schneemeyer, L. F.; Waszczak, J. V.; Siegrist, T.; Dover: R. B. v.; Rupp, L. W.; Batlogg, B.; Cava, R. J.; Murphy, D. W. *Nature* **1987**, *328*, 601−603.
(2) Vershinin, M.; Misra, S.; Ono, S.; Abe, Y.; Ando, Y.; Yazdani, A. *Science* **2004**, *303*, 1995−1998.
(3) Falck, L.; Lindqvist, O.; Mark, W. *Acta Crystallogr.* **1978**, *34B*, 1450−1453.
(4) Falck, L.; Lindqvist, O.; Moret, J. *Acta Crystallogr.* **1978**, *34B*, 896−897.
(5) Reinen, D.; Weitzel, H. *Z. Anorg. Allg. Chem.* **1976**, *424*, 31−38.
(6) Köhl, P.; Reinen, D. *Z. Anorg. Allg. Chem.* **1974**, *409*, 257−271.
(7) Iwanaga, D.; Inaguma, Y.; Itoh, M. *J. Solid State Chem.* **1999**, *147*, 291−295.

10.1021/ic0502832 CCC: $30.25
Published on Web 06/03/2005

conditions, according to the reaction eq 1. The starting materials were thoroughly ground and subsequently calcined at 650 °C in a muffle furnace in air for 3 days. Thereafter, the furnace was cooled to room temperature at a rate of 10 °C/h. $Na_2Cu_2TeO_6$ was formed as a green microcrystalline powder. For the single-crystal structure study, single crystals of green $Na_2Cu_2TeO_6$ were synthesized by heating the single-phase sample at 860 °C for 12 h, followed by slow cooling to room temperature.

$$Na_2CO_3 + 2CuO + TeO_2 + 1/2O_2 \rightarrow Na_2Cu_2TeO_6 + CO_2 \quad (1)$$

The sample was examined by powder X-ray diffraction using Cu $K\alpha_1$ radiation (INEL diffractometer with position sensitive detector) at room temperature and energy-dispersive X-ray analysis (EDAX), using the electron microscope LEO 1530 with an additional EDAX device, EDAX Pegasus 1200. No known compounds were detected in the X-ray powder pattern. The composition averaged over selected crystals using EDAX was Na:Cu:Te:O = 17(1):17(1):10(1):56 (in at. %). This is in quantitative agreement with the at. % values resulting from the single-crystal structure determination of 18.2:18.2:9.1:54.5.

Crystal Structure Determination. A block-shaped single crystal of $Na_2Cu_2TeO_6$ was selected for the data collection using the SMART Apex CCD with graphite-monochromatized Mo $K\alpha_1$ radiation (Bruker) at 200 K. A set of 725 frames (exposure time: 40 s) was collected up to $2\theta = 70°$. The data were corrected for Lorentz and polarization effects. Absorption corrections were based on fitting a function to the empirical transmission surface as sampled by multiple equivalent measurements using SADABS.[8]

The structure solution and refinements were performed with the SHELXTL program package.[9] The lattice parameters were indicative of monoclinic symmetry, and the systematic absences restricted the possible space groups to *C*2, *C*2/*m*, and *Cm*. The subsequent solution and refinement in *C*2/*m* were successful, and refining the model in *C*2 and *Cm* led to no improvements in the residual factors but instead resulted in high correlation factors. Crystallographic data, atomic coordinates, and thermal parameters, as well as selected bond distances for $Na_2Cu_2TeO_6$, are given in Tables 1−3.

Electronic Structure Calculation. We employed the WIEN2k package for the electronic structure calculations. This program package is based on the density functional theory and solves the Kohn−Sham equations with the full potential linearized augmented plane wave method.[10,11] Within this package, the generalized gradient approximation by Burke et al.[12] was utilized for the exchange-correlation energy. The calculations were performed both with and without spin polarization on the basis of 108 *k* points in the irreducible part of the first Brillouin zone of the primitive reciprocal cell. We abstained from performing antiferromagnetic calculations, as the magnetic cell is not known.

Resistance Measurement. We (cold-)pressed part of the ground phase-pure sample into a bar-shaped pellet of the dimensions 6 × 1 × 1 (in mm) for physical transport measurements, since no single crystals of sufficient dimensions were available. The high internal resistance of the pellet prevented Seebeck and electrical resistance measurements. On the basis of our experiences with other high-resistance materials, we conclude that its specific resistance must be above 1 MΩ cm at room temperature.

Magnetic Susceptibility Measurements. Variable-temperature magnetic susceptibility data for $Na_2Cu_2TeO_6$ were collected using a Quantum Design MPMS SQUID magnetometer. Both zero-field cooled (ZFC) and field-cooled (FC) data were obtained over the temperature range of 5−300 K at an applied field of 750 Oe. High-temperature (300−600 K) susceptibility data were collected using an oven insert at 17 500 Oe.

Table 1. Crystallographic Data for $Na_2Cu_2TeO_6$

empirical formula	$Na_2Cu_2TeO_6$
fw	396.66
temp	200(2) K
wavelength	0.710 73 Å
cryst system	monoclinic
space group	*C*2/*m* (No. 12)
a	5.7059(6) Å
b	8.6751(9) Å
c	5.9380(6) Å
b	113.740(2)°
V	269.05(5) Å^3
Z	2
D(calcd)	2.45 g/cm^3
abs coeff	6.67 mm^{-1}
F(000)	180
cryst size	0.04 × 0.04 × 0.02 mm
θ range for data collcn	3.75−35.00°
reflcns collcd	1471
indpndt reflcns	605 [R(int) = 0.0533]
refinement method	full-matrix least squares on F^2
data/restraints/params	605/0/31
goodness-of-fit on F^2	1.068
R indices (all data)	R1 = 0.0314, wR2 = 0.0823
extinctn coeff	0.010(1)
largest diff peak and hole	3.10 and −1.93 e/Å^3

Table 2. Atomic Coordinates and Equivalent Displacement Parameters

atom	site	x	y	z	U_{eq}[a]/Å^2
Te	2a	0	0	0	0.00490(1)
Cu	4g	0	0.66475(4)	0	0.0069(2)
Na	4h	0	0.1839(2)	1/2	0.0111(3)
O1	8j	0.1936(5)	0.1632(2)	0.2121(5)	0.0076(4)
O2	4i	0.7574(5)	0	0.1640(5)	0.0078(4)

[a] U_{eq} is defined as one-third of the trace of the orthogonalized $\mathbf{U}_{ij}$ tensor.

Table 3. Selected Bond Distances (Å) for $Na_2Cu_2TeO_6$

Te−O1 4×	1.921(2)	Cu−Cu 1×	2.858(1)
Te−O2 2×	1.988(3)	Cu−Cu 2×	3.214(1)
Cu−O1 2×	1.978(2)	Na−O1 2×	2.309(2)
Cu−O2 2×	1.999(2)	Na−O1 2×	2.386(3)
Cu−O1 2×	2.533(4)	Na−O2 2×	2.494(2)

Results and Discussion

Crystal Structure. $Na_2Cu_2TeO_6$ is a new quaternary layered transition-metal oxide crystallizing in a new structure type. The assignment of formal charges is straightforward, yielding fully oxidized cations Na^I and Te^{VI} and, therefore, Cu^{II}. This type is a (filled) distorted substitution variant of the CdI_2 type, with the O anions forming layers reminiscent of the hexagonal closest packing. The Cd atoms are substituted by the Cu and Te cations, and the Na cations fill pseudooctahedral voids between the $^2_\infty[Cu_2TeO_6]$ layers (Figure 1).

(8) *SAINT*, version 4 ed.; Siemens Analytical X-ray Instruments Inc.: Madison, WI, 1995.
(9) Sheldrick, G. M. *SHELXTL*, version 5.12 ed.; Siemens Analytical X-ray Systems: Madison, WI, 1995.
(10) Blaha, P.; Schwarz, K.; Madsen, G. K. H.; Kvasnicka, D.; Luitz, J. *WIEN2k, An Augmented Plane Wave + Local Orbitals Program for Calculating Crystal Properties*; Techn. Universität Wien: Wien, Austria, 2001.
(11) Schwarz, K. *J. Solid State Chem.* **2003**, *176*, 319−328.
(12) Perdew, J. P.; Burke, K.; Ernzerhof, M. *Phys. Rev. Lett.* **1996**, *77*, 3865−3868.

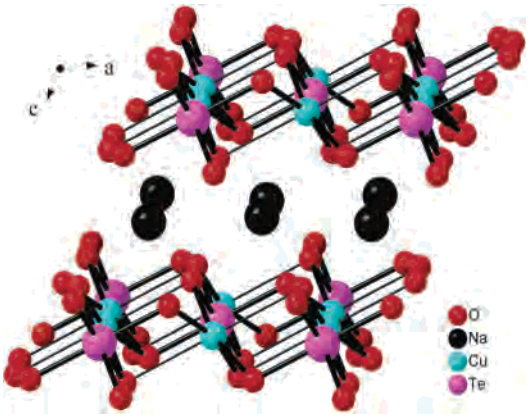

Figure 1. Crystal structure of $Na_2Cu_2TeO_6$.

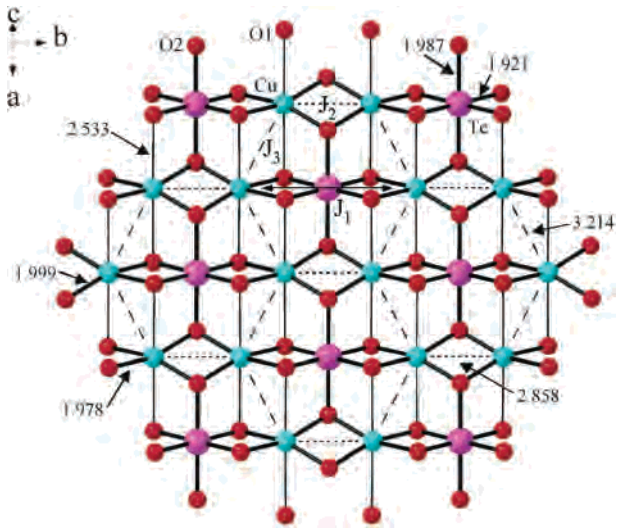

Figure 2. $^2_\infty[Cu_2TeO_6]$ layer of $Na_2Cu_2TeO_6$.

The NaO_6 octahedra exhibit an $AlCl_3$-like arrangement with Na−O bonds between 2.31 Å and 2.49 Å. Utilizing the Brown−Altermatt equation for the bond valences s, $s = \exp[(r_0 - r)/0.37\ \text{Å}]$, with $r_0 = 2.527$ Å for Na−O bonds and r being the actual bond distance,[13] we obtain a total valence of 1.23 for the Na atom. A $^2_\infty[Cu_2TeO_6]$ layer is depicted in Figure 2, revealing the substitution pattern of two Cu cations and one Te cation for the Cd atoms of CdI_2. The TeO_6 polyhedron is an almost regular octahedron, with six Te−O bonds between 1.92 Å and 1.99 Å. Such bond lengths are expected for Te^{VI} oxides, as also found in Na_2TeO_4 (Te−O bonds between 1.85 and 2.04 Å)[14] and $CuTeO_4$ (1.87−2.02 Å).[3] Using $r_0 = 1.917$ Å for Te−O bonds, we calculate a valence of 5.65 for the Te atom in $Na_2Cu_2TeO_6$. On the other hand, significant deviations from the octahedral coordination of the Cu cation are obvious, as it forms four short (2.00 Å) and two longer (2.53 Å) Cu−O interactions. Deviations such as this, toward an elongated octahedron, are typical for Cu^{II} oxides; e.g. tenorite, CuO, comprises four bonds in the range 1.94−1.97 Å and two longer contacts of 2.82 Å.[15] Other examples include the superconducting cuprates. Overall the Cu atom of $Na_2Cu_2TeO_6$ exhibits a valence of 1.93 (calculated using $r_0 = 1.679$ Å), very close to the postulated value of 2.

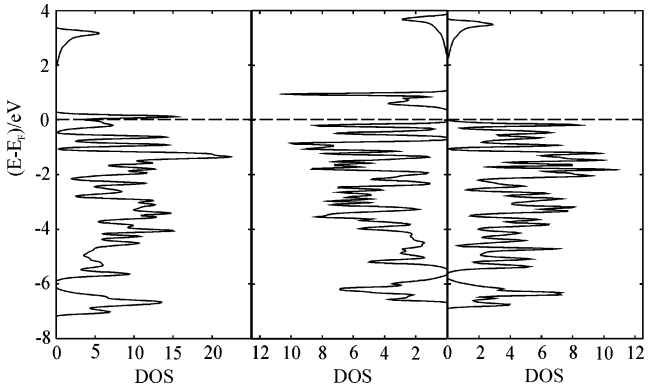

Figure 3. Densities of states of $Na_2Cu_2TeO_6$: (left) non-spin-polarized; (center) spin-up; (right) spin-down. Dashed horizontal line: Fermi level.

The CuO_6 polyhedra are linked to three CuO_6 and three TeO_6 neighbors via edge-sharing. This results in one Cu−Cu contact/Cu^{II} of 2.86 Å and two of 3.21 Å (dashed lines in Figure 2), yielding a distorted honeycomb lattice of Cu atoms.

Electronic Structure. The non-spin-polarized densities of states (left) and the spin-up (center) and spin-down (right) densities of states (DOS) of the spin-polarized calculation are depicted in Figure 3. The filled valence orbitals are O-2s (occurring below the energy window shown), O-2p, and Cu-3d orbitals. Per Cu^{II} atom, there are four filled 3d bands and one half-filled 3d band. This amounts to two half-filled bands, as there are two Cu atoms in the first Brillouin zone, energetically overlapping in the non-spin-polarized calculation. Upon spin-polarization, the latter split into filled (spin-up) and empty (spin-down) states; i.e., a gap opens.

The Cu-d bands, dominating the area between −2 eV and the Fermi level, are separated from the unfilled Te-5s-based bands by a significant gap, e.g. 1.7 eV in the non-spin-polarized DOS. The gap between the filled O-2p bands and Te-5s is above 4 eV. We assume the green color of this material stems from d−d transitions and/or possible Cu-d to Te-s charge transfer.

Physical Properties. We were unable to measure the value of the electrical resistance because it was too high to be determined (at room temperature). The magnetic data, on the other hand, are of special interest since the WIEN2k calculations yielded a significant spin polarization. Examination of the high-temperature data of the inverse magnetic susceptibility (Figure 4) shows adherence to the Curie−Weiss law from 400 to 600 K with a temperature-independent (Pauli) paramagnetic term (χ_{TIP}), $\chi = C/(T - \Theta) + \chi_{TIP}$. The fitting parameters found are $\chi_{TIP} = 4.0(3) \times 10^{-4}$ emu/mol, the Curie constant, $C = 0.855(8)$ emu/mol K, and the Weiss constant, $\Theta = -87(6)$ K. The Curie constant is consistent with a "spin-only" effective magnetic moment, μ_{eff}, of 1.85(2) μ_B/Cu^{II} ($S = 1/2$). This gives a Lande g-factor of 2.14(1) for this compound, which is within the range expected for Cu^{II}.

(13) Brown, I. D.; Altermatt, D. *Acta Crystallogr.* **1985**, *B41*, 244−247.
(14) Kratochvil, B.; Jensovsky, L. *Acta Crystallogr.* **1977**, *33B*, 2596−2598.
(15) Calos, N. J.; Forrester, J. S.; Schaffer, G. B. *J. Solid State Chem.* **1996**, *122*, 273−280.

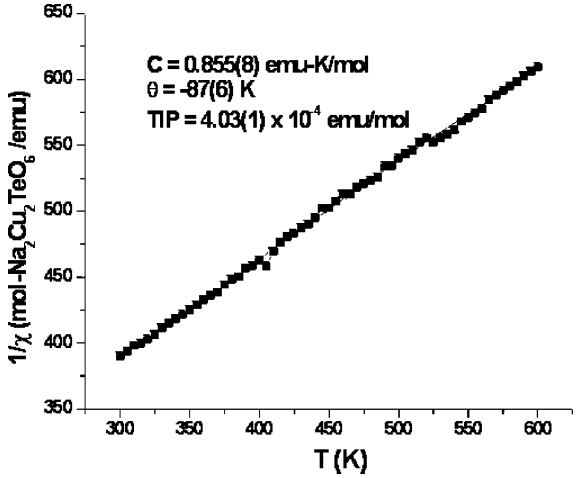

Figure 4. Inverse magnetic susceptibility of $Na_2Cu_2TeO_6$ between 300 and 600 K. A fit to the Curie−Weiss law plus a TIP term was done over the interval from 400 to 600 K, yielding the parameters shown.

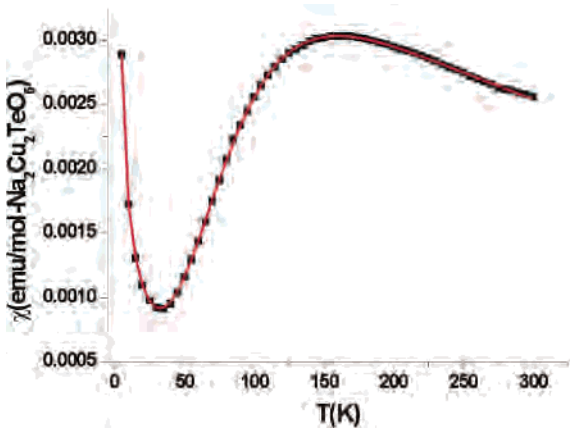

Figure 5. Dc magnetic susceptibility (ZFC) of $Na_2Cu_2TeO_6$ between 5 and 300 K. The solid line is a fit to a three-component function including an alternating $S = 1/2$ chain model, a TIP term, and a Curie−Weiss term to model the low-temperature upturn as discussed in the text. The fitted parameters are given in Table 5.

Table 4. Relative Strengths of Cu−Cu Exchange Pathways (Figure 2) in the *a,b* Plane of $Na_2Cu_2TeO_6$

path	symbol	$(\Delta e)^2$ [$(meV)^2$]	rel magnitude
SSE-b	J_1	10200	1
SE-b	J_2	3320	0.33
SE-inter	J_3	130	0.01

Table 5. Comparison of the Fitting Parameters for the Simple Dimer (Bleaney−Bowers) Model and the Alternating Chain Model with $J_2/J_1 = 0.10(1)$

model	*g*	*J*/*k* (K)	J_2/J_1	TIP	*C*	Θ (K)
dimer	2.02(1)	−130.1(2)	0	0.000 60(1)	0.010(3)	0.72(14)
alt chain	2.03(1)	−134.6(3)	0.10(1)	0.000 66(2)	0.0070(4)	1.2(2)

The Cu^{II} ions lie in the *a,b* plane. Three interaction pathways are to be considered (Figure 2). Two of these involve a linear chain along the *b*-axis, J_1 and J_2, and one interchain pathway, J_3. J_1 involves a super-superexchange pathway, Cu−O−Te−O−Cu, designated SSE-b with a Cu−Cu distance of 5.82 Å and a Cu−O···O angle of approximately 139°. J_2 corresponds to a Cu−O−Cu linkage with a considerably shorter Cu−Cu distance of 2.86 Å and a Cu−O−Cu angle of 91.3°, SE-b. Last, J_3 also involves a Cu−O−Cu pathway with Cu−Cu = 3.21 Å and a Cu−O−Cu angle of nearly exactly 90°, SE-inter. The spatial dimensionality of the short-range order depends on the relative magnitudes of the three exchange constants. For example, if $J_2 \approx J_3 \gg J_1$, then the correlations would be two-dimensional in the form of a distorted honeycomb lattice. If $J_1 \approx J_2 \gg J_3$, then one expects a linear chain model, which may be an alternating chain depending on the ratio J_1/J_2. Finally, if this ratio were to become vanishingly small, a simple dimer or zero-dimensionality model would be obtained.

To aid in determining these relative magnitudes, the method of magnetic dimer analysis was applied.[16] We utilized the extended Hückel[17,18] model to calculate the interactions between the magnetic orbitals (Δe), and the exchange constants are estimated from the expression $J \approx -(\Delta e)^2/U_{eff}$. As U_{eff} is constant for a given magnetic ion, the trend in Δe is a semiquantitative representation of the trend in *J*. The magnetic orbitals are taken as the $d_{x^2-y^2}$ orbitals of Cu^{II}. The results are presented in Table 4. The Te orbitals were not included in the calculation of J_1.

Clearly, J_3 can be ignored, thus eliminating the honeycomb lattice model. The small value of J_3 can be understood in terms of the spatial relationship of the magnetic $d_{x^2-y^2}$ orbitals, which lie in the CuO_4 plane involving the short Cu−O distances. These planes are essentially parallel in the J_3 dimer (Figure 2). The large value of J_1 may be attributed to the good overlap geometry of the Cu−O−O−Cu linkage. The Cu−O−Cu angle of 90° can explain the relatively small J_2 value.

At this stage an alternating chain model appears to be appropriate. Therefore, the data were first fit to the published function[19] beginning with $J_2/J_1 = 0.3$. In addition to the expression for the alternating chain, a Curie−Weiss term, $C/(T - \Theta)$, was included to account for the low-temperature upturn as well as a temperature-independent term (TIP). This model refined to $J_2/J_1 = 0.10(1)$, shown in Figure 5, which now suggested that a simple dimer (Bleaney−Bowers) model[20] should also be tried.

A fit was attempted using this model yielding a very similar result. The fitting parameters for the two models are compared in Table 5, suggesting that they are nearly equivalent. However, a further test comparing the low-temperature fits to the data on the two models (Figure 6) indicates that the alternating chain model appears to be slightly better. This is reasonable as only at low temperatures will the effect of a small but finite J_2 be manifest.[21] In conclusion, the magnetic short-range order in $Na_2Cu_2TeO_6$

(16) Whangbo, M. H.; Koo, H. J.; Dai, D. *J. Solid State Chem.* **2003**, *176*, 417−481.
(17) Hoffmann, R. *J. Chem. Phys.* **1963**, *39*, 1397−1412.
(18) Whangbo, M.-H.; Hoffmann, R. *J. Am. Chem. Soc.* **1978**, *100*, 6093−6098.
(19) Hall, J. W.; Marsh, W. E.; Weller, R. R.; Hatfield, W. E. *Inorg. Chem.* **1981**, *20*, 1033−1037.
(20) Bleaney, B.; Bowers, K. D. *Proc. R. Soc. (London)* **1952**, *A214*, 451−465.
(21) He, Z.; Kyomen, T.; Itoh, M. *Phys. Rev.* **2004**, *B69*, 220407.

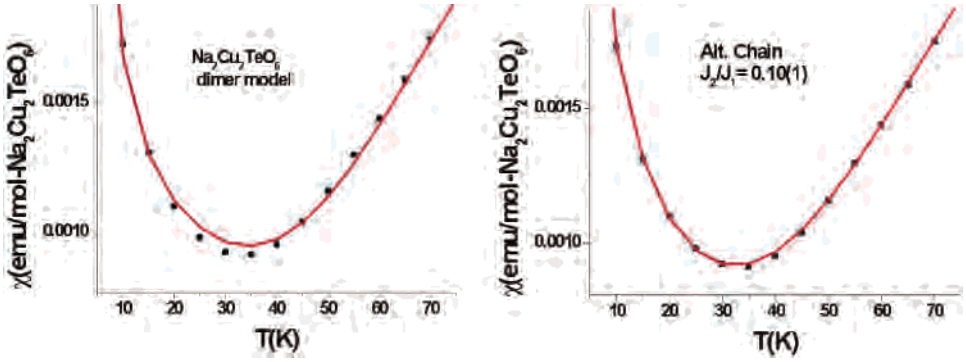

Figure 6. Comparison of the low-temperature fits for the single dimer model ($J_2/J_1 = 0$) (left) and the alternating chain model with $J_2/J_1 = 0.10$ (right).

is best described as weakly one-dimensional, an alternating chain with $J_2/J_1 \approx 0.1$, although the zero-dimensional dimer model is nearly as good.

Finally, it is possible to estimate the so-called "spin gap", Δ, which is the effective energy difference between the ground singlet, $S = 0$, state and the lowest excited triplet state, $S = 1$, from recent theory.[22] The result for $J_2/J_1 = 0.10$ gives $\Delta = 0.9463J_1 = 127$ K. Thus, one would not expect long-range order to develop in this material at low temperatures.

(22) Barnes, T.; Riera, J.; Tennant, D. A. *Phys. Rev.* **1999**, *B59*, 11384−11397.

Acknowledgment. Financial support from the NSERC, CFI, OIT (Ontario Distinguished Researcher Award for H.K.), the Province of Ontario (Premier's Research Excellence Award for H.K.), and the Canada Research Chair program (CRC for H.K.) is appreciated. We thank Dr. P. Dube and Ms. A. Sefat for assistance with the SQUID magnetometer measurements at the Brockhouse Institute for Materials Research at McMaster University.

Supporting Information Available: One X-ray crystallographic file (CIF). This material is available free of charge via the Internet at http://pubs.acs.org.

IC0502832